CrossMark

Reconstruction of glacier fluctuations in the East Sayan, Baikalsky and Kodar Ridges (East Siberia, Russia) during the last 210 years based on high-resolution geochemical proxies from proglacial lake bottom sediments

O. G. Stepanova[1] · V. A. Trunova[2] · V. V. Zvereva[2] · M. S. Melgunov[3] · A. P. Fedotov[1]

Abstract We have presented results of study of bottom sediments of the proglacial lakes enriched with meltwater of Peretolchin Glacier (the East Sayan Ridge), Chersky Glacier (the Baikalsky Ridge) and glaciers of the Kodar Ridge. Bottom sediments formed from the end of the Little Ice Age to 2013 were investigated with time resolution in year-season, using X-ray fluorescence with synchrotron radiation and inductively coupled plasma mass spectrometry. Depth–age models of the cores were estimated from year laminate layers, using ^{210}Pb and ^{137}Cs chronology. Intense glacier thawing was calculated from the amount of clastic matter supplied by glacier meltwater into proglacial lakes. A high content of some elements was closely associated with clastic material (e.g. Rb, Zr, Nb, Y or Th) in bottom sediments, and most likely these elements affected the intensity of glacier melting. We have defined three periods in significant increase of glacier flow/melting during the last 210 years. The first period (ca. 1800–1890), supply of suspended material by meltwater into Lake Ekhoy (the East Sayan Ridge) and Lake Preobrazhenskoe (the Kodar Ridge), was not intense until 1850 and 1875, respectively. However, the rate of meltwater supply into Lake Izumrudnoe (the Baikalsky Ridge) was high during the Little Ice Age, and it is likely attributed to local moisture from Lake Baikal. The regional glacier water balances were most likely positive during the second period (ca. 1890–1940). The third period (ca. 1940–till present) was characterised by moderate melting rate of glaciers located on the Kodar and Baikalsky Ridges, in contrast to Peretolchin Glacier that demonstrated the highest rate of melting and changes in outlines during this period.

Introduction

Mountainous and highland regions are highly sensitive to local climate change (Hoelzle et al. 2007; Owen et al. 2009). Small mountain glaciers exist in a sensitive state of equilibrium with climate and are therefore good indicators of climate change (Haeberli et al. 2004; Paul 2002; Solomina et al. 2008). The slightest change in climate (precipitation and temperature) can affect the overall mass balance of the glacier (Dyurgerov and Meier 2000). A large contribution of the catchment runoff is derived from ice meltwater and snowmelt water (Zhao et al. 2013; Nie et al. 2013; Wang et al. 2015). At the same time, glaciers located in the continental areas far from the main sources of moisture are the most sensitive to climate changes.

This study was conducted in the south-eastern part of East Siberia (Russia). This region is very sensitive to moisture regime as it is located in the margin area, when moisture from the North Atlantic is strongly depleted, and the penetration of the East Asian monsoon is weak and rare (Kuznetsova 1978). In winter months, the Siberian anticyclone strongly blocks and reduces all external influences on the region (An 2000). Therefore, at present the areas of

✉ O. G. Stepanova
sog@lin.irk.ru

[1] Limnological Institute of the Siberian Branch of RAS, Ulan-Batorskaya street 3, Irkutsk, Russia

[2] Nikolaev Institute of Inorganic Chemistry of the Siberian Branch of RAS, Novosibirsk, Russia

[3] Institute of Geology and Mineralogy of the Siberian Branch of RAS, Novosibirsk, Russia

glaciers in mountains of East Siberia are rather small (Margold and Jansson 2011). In most cases, these glaciers are less than 1 km² (Avsiuk and Kotlyakov 1967; Stokes et al. 2013; Osipov and Osipova 2014). However, alpine relief and other geomorphological evidences such as terminal moraines, fossil shorelines and deltas of glacial lakes indicate extensive glaciation of the area in the past (Back and Strecker 1998; Osipov et al. 2003; Solomina 2000; Osipov and Khlystov 2010). For example, glaciers covered about 13,000 km² around Lake Baikal during the Last Glacial Maximum (Osipov and Khlystov 2010).

According to the recent studies (Stoetter et al. 1999; Nesje and Dahl 2001; Yang et al. 2008), glacier fluctuations in the Northern Hemisphere were not synchronous during the Late Holocene. There are numerous papers devoted to the Late Holocene climatic changes in Europe, Fennoscandia and Canada (e.g., Jones et al. 2009 and their references). However, the information on fluctuations of East Siberian glaciers during the Late Holocene and, in particular, the last few centuries is still scarce. Observation of East Siberian glaciers started relatively not long ago: the first galciers were described in the mid-nineteenth century. Glaciers located in the East Sayan Ridge were firstly described by Peretolchin in 1896–1903 (Peretolchin 1908). Glaciers of the Baikalsky Ridge were discovered recently by Aleshin (1982). The first glacier inventory of the Kodar Ridge was published by Preobrazhenskiy (1960), which consisted of 31 glaciers. To date, the inventory of East Siberian glaciers is based on comparison of satellite images (mainly of those in the 2000s) with the 1960s glacier inventory of the USSR (Kitov et al. 2009; Shahgedanova et al. 2011; Stokes et al. 2013; Osipov et al. 2013; Osipov and Osipova 2014).

Proglacial lakes are of great significance for the Quaternary record. The character and behaviour of proglacial lakes depend on surface energy balance, dynamics of glaciers, glacial meltwater and sediment fluxes (e.g., Gardelle et al. 2011; Larsen et al. 2011; Carrivick and Tweed 2013). Considerable progress has been made in the analysis of bottom sediments from proglacial lakes, which are used to reconstruct former glacier activity (Karlen and Matthews 1992; Dahl et al. 2003). It allowed the development of high-resolution quantitative continuous records for glacier advance and retreats (Lie et al. 2004; Rosqvist et al. 2004; Nesje et al. 2008; Bakke et al. 2005).

The goal of the present paper was to reconstruct a glacier response to climate changes during the last 210 years based on high-resolution geochemical proxies inferred from the proglacial lakes of the East Sayan Ridge (ESR), the Baikalsky Ridge (BR) and the Kodar Ridge (KR). Records of this period bear critical information on significant climate changes, e.g. the transition from LIA to the

Recent Warming (RW) and the beginning of anthropogenically forced global warming.

Regional setting

Peretolchin Glacier (ESR) is located at Mount Munku-Sardyk 3491 m above sea level (a.s.l.) on the Russian–Mongolian border, the highest peak of ESR. In 1893–1903, the glacier was about 0.68 km², length about l.5 km, and upper and lower boundaries covered from 3050 to 2776 m a.s.l., respectively (Peretolchin 1908). In 2006, the glacier was about 0.3 km², length about 1 km, and upper and lower boundaries were from 3490 to 2937 m a.s.l., respectively (Osipov et al. 2013). The proglacial Lake Ekhoy (51.44°N, 100.36°E) is located at 2613 m a.s.l., area of about 0.033 km², 1.1 km to the north of the glacier.

Chersky Glacier (BR) is located in an alpine-type terrain near Mount Chersky (2588 m a.s.l.), about 18 km to the west of the northern basin of Lake Baikal (Fig. 1). In 1982, the glacier was about 0.6 km², ice thickness 40–50 m, length about l km, and upper and lower boundaries continued from 2020 to 1750 m a.s.l., respectively (Plyusnin et al. 2008). In 2011, the area was 0.4 km², upper and lower boundaries from 2138 to 1796 m a.s.l., respectively (Osipov and Osipova 2014). The proglacial Lake Izumrudnoe (55,03°N, 108,43°E) is a small freshwater lake with an area of about 0.05 km², situated at 1460 m a.s.l. and 0.7 km to the east of the glaciers. The major source of water for this lake is an outflow of meltwater from the glacier (Fig. 1).

Sygyktinskiy (SU5D17201005-east) and Kolosov (SU5D17201006) Glaciers (KR) are situated on the high mountain Kodar Ridge on the northeast edge of the Baikal Rift Zone (Fig. 1). In 2009, the areas were 0.31 and 0.42 km², upper and lower boundaries changed from 2679/2444 and 2585/2289 m a.s.l., respectively (Osipov and Osipova 2014). Lake Preobrazhenskoe (56,50°N, 117,26°E) is located at 2268 m a.s.l, an area of about 0.045 km², 0.6 km to the east of the Sygyktiskiy and 0.3 km to the west of the Kolosov.

These proglacial lakes are fed by surface inflows several small and shallow (about 20–30 cm) streams: 5 streams into Lake Ekhoy and 8 streams into Lake Izumrudnoe. It is obvious these streams are not enough strong for effective transport of suspended particle through deep proglacial lake to the outflow, although some portion of very fine size particles (less than pelite) is outflowed from the lakes. Water transparency of the studied lakes is 2–3 m because of high turbidity.

The climate in this region of East Siberia is continental: large differences in the mean January (−30 °C) and mean
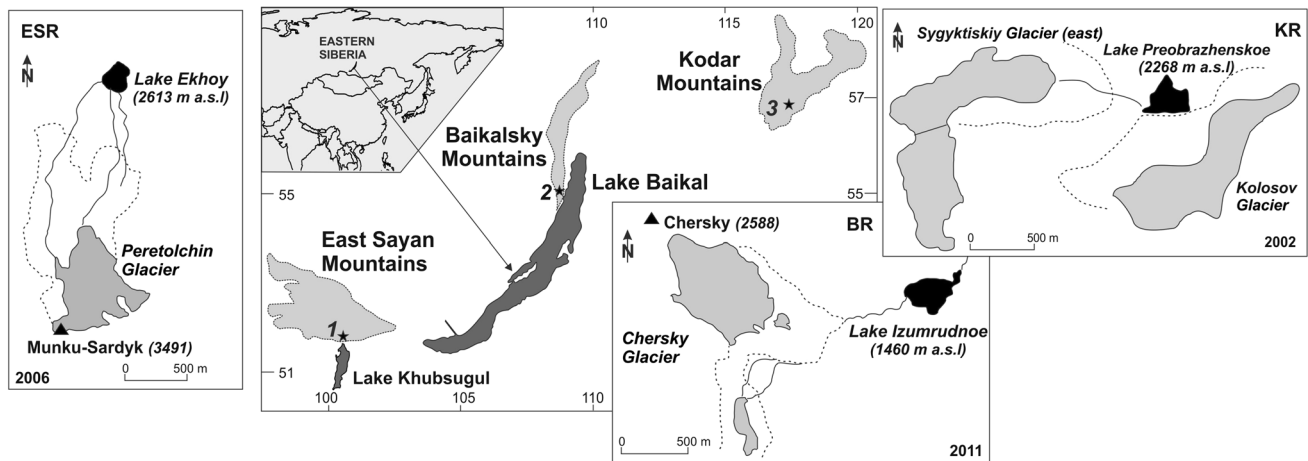
Fig. 1 The locations of proglacial Lakes Ekhoy (1), Izmrudnoe (2), and Preobrazhenskoe (3). *Grey areas and dotted lines* outlines and recent terminal moraines (the LIA) of glaciers

July (15 °C) temperatures. Annual precipitation is relatively low ranging from 220 to 590 mm (NOAA dataset ftp://ncdc.noaa.gov/pub/data). The vegetation around the studied lakes is represented by grass-moss and shrubs.

Methods

In 2012–2013, sediment cores were taken from the central part of Lake Ekhoy (ESR) (83 cm long at a depth of 16 m), the central part of Lake Preobrazhenskoe (KR) (31.5 cm long at a depth 17 m) and Lake Izmrudnoe (BR) (15 cm long at a depth of 14 m), using a Uwitec Corer sampler.

The colour core photos were processed with the program Strati-Signal 1.0.5 (Ndiaye et al. 2012) with the 0.02–0.03 mm discreteness of the analysis of image colour components. It is obvious that there is a strong season dynamics of suspended material supply into small high altitude proglacial lakes by streams. The supply of coarse grain size material in a short ice-free period is sharply blocked due to rapid freezing of small tributaries of proglacial lakes. As a result, there is some colour contrast between summer and winter sediment layers. A colour pattern of core sediments was used to calculate the annual layers using the Strati-Signal 1.0.5.

The cores were dated using ^{210}Pb and ^{137}Cs chronology. The content of ^{238}U, ^{234}Th, ^{226}Ra, ^{137}Cs and ^{210}Pb in the studied samples was measured using a high-resolution semiconductor gamma-spectrometry technique (Melgunov et al. 2003; Gavshin et al. 2005). Low-energy gamma lines were used as analytical signals: 46.5 keV for ^{210}Pb, 63.3 and 92 keV for ^{238}U (by ^{234}Th) and 186.1 keV for ^{226}Ra. The measurements were performed on a EURISYS MEASURES low background well-type HPGe detector EGPC192-P21-R with an active volume of 220 cm^3,

relative efficiency—50 %, FWHM (1,332 keV)—2.1 keV. The counting time was 48 h for each sample. It was chosen in order to obtain a statistical error due to the random process of decays not worse than 5 % for all analytical γ lines. The detection limits for ^{137}Cs, ^{210}Pb, ^{234}Th and ^{226}Ra in the measured samples were of the order of 0.02 Bq. We calculated the depth–age relationship for the uppermost 15 cm using the constant rate of supply (CRS) model (Binford 1990). ^{210}Pb was found in the sediments first in a ''supported'' form by in situ production from ^{238}U or ^{226}Ra decay, at equal activity to its parent nuclides, which is normally assumed to be constant downcore. The second fraction, the ''unsupported'' or excess ^{210}Pb (^{210}Pb$_{excess}$), was of atmospheric origin. Atmospheric ^{210}Pb entered the aquatic environments by direct deposition with rain and also by runoff and erosion from catchment areas. Excess ^{210}Pb concentrations were calculated by ^{226}Ra.

The elemental composition of the core was investigated by two methods: X-ray fluorescence spectrometry (XRF-SR) for quantitative analysis of 20 trace elements (from K to U) and inductively coupled plasma mass spectrometry (ICP-MS). The scanning analysis was performed at an original XRF beamline of the VEPP-3 storage ring (Budker Institute of Nuclear Physics, Novosibirsk, Russia) (Trounova et al. 1998). The 15 keV band was used for the determination of elements from K to Br. The 25 keV band was used to determine Rb, Sr, Y, Zr, Nb, Mo, Th and U. The 42 keV band was used for the determination of Cd, Sn, Sb, I, Ba, La and Ce. The samples were 22 cm long, 1.2 cm wide and 0.6 cm thick were placed into aluminium trays. The trays were moved vertically under a 1 mm (sampling resolution) and SR beam collimated by a cross-slit system (Zolotarev et al. 2001). The spectral responses of the absolute concentrations of elements from their fluorescent peaks were processed using the algorithm of fundamental

parameters to overcome problems caused by water content variability in nearly saturated wet sediments (Phedorin and Goldberg 2005). In addition to XRF-SR, the elemental composition of the Ekhoy core was studied using ICP-MS with a sampling resolution of 1 cm. ICP-MS was performed as described by Zhuchenko et al. (2008). A distinct in detected of some elements by these methods was described by Phedorin et al. (2000a) and Zhuchenko et al. (2008). "Light" elements (e.g. Br, I, Cu, etc.) are practically inaccessible for determination by ICP-MS, or Ti, Be, Sn, Hf and Zr are poorly extracted from sediment samples at treatment by acids. However, ICP-MS did not used for other cores because time resolution will be low at sampling resolution of 0.5 or 1 cm. In our figures, we have only shown the distribution of elements closely associated with clastic material, weathering and the major axes of a principal components analysis. We do not consider in detail the elements of the markers of bioproductivity (Vorobyeva et al. 2015) and diagenesis (e.g. Br, Fe, and Mn et al.) because our aim is to reconstruct the suspended matter transported into proglacial lakes.

Statistical analyses were carried out using a principal component analysis (PCA), then redistributed using the varimax rotation method and CONISS analysis using a square-root transformation by the R package rioja (Juggins 2012).

Results

Core Ekhoy (ESR)

A texture of bottom sediments was most likely similar to a laminar texture. Light layers enriched with sand and coarse silt formed most likely in summer form a suspended material of surface inflows. A thickness of these layers varied from 0.2 to 7 mm, the bottom boundaries of these layers

were clear. These "sand" layers were overlapped by fine grey-green silty clay layers up to 1 mm thick (Fig. 2). We assumed that these "clay" layers were formed during ice-covered periods. Colour transitions between "sand" and "clay" layers were well detected by a digital image processing (Fig. 2). However, this laminate texture occurred clearly only in the upper part (0–25 cm below sediment surface, bss) of the core.

According to the CRS-model, the sediment interval in 24–25 cm bss formed after 1844. We extrapolated linearly the average sediment accumulation rate in the core interval of 20–25 cm down to 35 cm bss, and the calculated age was ca. 1800. The sediment interval 5–6 cm bss was dated as 1979 and there was a well-resolved peak of ^{137}Cs at this interval. It is likely linked to the Chernobyl accident of 1986. We improved the time-resolution of the CRS-model for the core interval in 0–25 cm bss by a depth–age model based on counting of annual layers (Fig. 2).

The PCA analysis showed that axes 1 and 2 explained 49.8 and 32.3 % of the variability of the elemental composition, respectively (Fig. 2). We did not found that any PCA axis could be clearly attributed to the elements typical of the clastic material, high-mobility elements or organic materials. For example, the PCA-1 axis was characterised by a negative correlation between Mo, P, Ni, Cr, Y, Yb and Sr, K, Nb. The PCA-2 axis was formed by U, Sm, Nd, Ca, Ti, Fe, Zn, Mn, Th and Pb.

We divided the elemental and mineralogical records of interval core formed since ca. 1800 (0–35 cm bss) into five zones (1–5). Zone 1 (35–29.5 cm bss, ca. 1800–1862) was characterised by a moderate low content of detected elements (Fig. 2). Zone 2 (29.5–22 cm bss, 1850–1906), beginning at 29 cm and moving upward, revealed a drastic increase of the element content (in particular K and Nb). In Zone 3 (22–13.5 cm bss, 1906–1946), the content of elements typical of the clastic material (e.g. Th, Rb or Nb) gradually increased since 1930, but this tendency was not
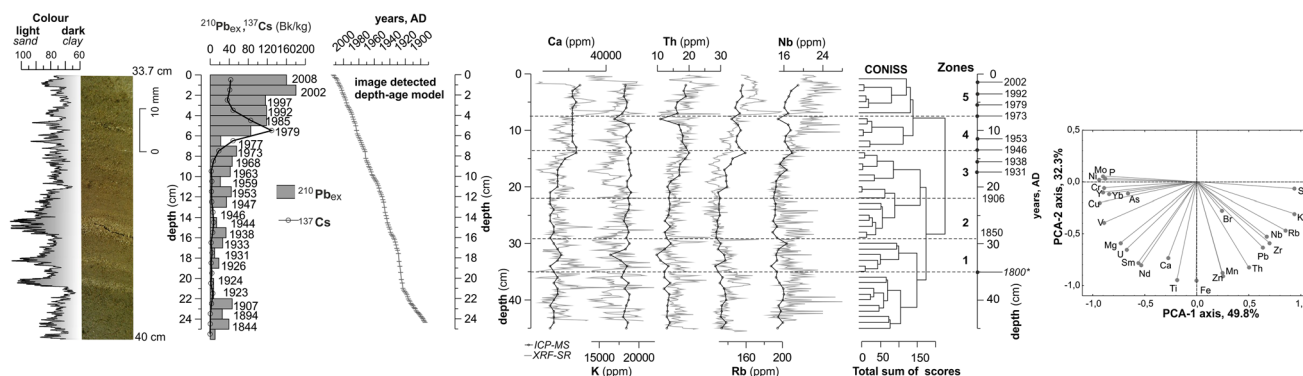
Fig. 2 Core Ekhoy (East Sayan):- colour processing of the core photos, the depth–age model based on (1) radioactive isotopes ^{210}Pb and ^{137}Cs and (2) counting of annual layers, the distributions of some elements in the sediments (biplot for the first two principal components, ICP-MS data)

clear for high-mobility elements (e.g. Ca or K) (Fig. 2). In Zone 4 (13.5–7 cm bss, 1946–1973), the contents of practically all elements. In particular, the content of elements typical of the clastic material increased significantly. Zone 5 (7–0 cm bss, from 1973 to the present) contained the highest concentration of all elements. Beginning from ca. 2000, their content drastically decreased.

Lake Izumrudnoe (BR)

Bottom sediments were composed of fine laminate grey-green silty clay with a thickness from 0.1 to 0.4 mm and sand–silty layers with a thickness up to 0.8 mm. Unlike the layers in the core Ekhoy, these layers enriched with sand are dark, as a result summer layers are darker in colour diagram. Excess of ^{210}Pb reached around 2–5 Bq kg^{-1} at 9–10 cm bss, and was negative below 10 cm bss (Fig. 3). According to the CRS-model, the sediment interval in 8–9 cm bss was formed after 1849. The well-resolved peak of ^{137}Cs at 1–2 cm bss was likely linked to the Chernobyl accident of 1986, and, according to ^{210}Pb chronology, this interval was dated 1994. However, this offset could be explained by a high ability caesium to migration. We extrapolated the sediment accumulation rate down to 11 cm bss and calculated that 10.7 cm bss was ca. 1800.

The principal component analysis showed that axes 1 and 2 explained 60 and 17.2 % of the variability of the elemental composition, respectively (Fig. 3). The first axis included both high-mobility elements (e.g. Fe, K, Mn et al.) and trace elements typical of the clastic material (e.g. Ti, Rb, Y, Th et al.). The second axis was likely associated with elements (e.g. Cu, Pb, U or Mo) easily incorporated into organic materials or secondary iron and manganese oxides that flocculated and precipitated onto clay-size aluminosilicates (e.g. Mo, Zr and Nb).

According to the CONISS analysis, the elemental records were likely divided into four zones. Zone 1 was formed about 1800–1910 (10.7–8 cm bss) and

characterised by a high content of elements, in particular Th, Rb and K (Fig. 3). The content of elements decreased in the 8–5 cm bss interval (zone 2, 1910–1940) of the core. The content of elements described by the PCA-1 axis decreased more vividly than elements of the PCA-2 axis. In Zone 3 (5–2.7 cm bss, 1940–1990), the content of all elements associated with the PCA-1 axis increased while the elements of the PCA-2 axis moderately decreased (Fig. 3). In Zone 4 (2.7–0 cm bss, 1990- till present), the content of Ca, Ti, Th and Nb significantly increased and minor changes were recorded in the content of K, Rb and Cu. In the upper part of the core, the content of all elements dramatically decreased.

Lake Preobrazenskoe (the Kodar Ridge)

The upper part (0–15 cm bss) of the core consisted of two types of sediments. Fine light-brown silty clay was visualised at the bottom of the core (15–4 cm). Beginning from 4 cm and moving upwards, the colour gradually changed to olive grey. Laminate texture was not recorded along the studied interval (Fig. 4). The upper 1.4 cm part of the core contained much water; therefore, we united the interval in one sample to increase weight of this sample. Excess of ^{210}Pb concentration had negative values below 7 cm bss. The sediment interval in 5–6 cm was dated 1864 (Fig. 4). The ^{137}Cs dates did not show two typical peaks characteristic of the fallout from nuclear weapon testing (1963) and from the Chernobyl incident (1986). ^{137}Cs gradually increased beginning from 4 to 5 cm bss to the upper part of the core.

The PCA-1 axis, which accounted for 36 % of the total variation of the element composition, had a large loading for Th, Pb, Y, Nb, Ni, Br, U and Sr. Interestingly, negative correlation was recorded between the distribution of Br and U (Fig. 4). The PCA-2 axis, which accounted for 20.3 % of the total variation, had a large loading for elements with high migratory capacity and ability to form soluble
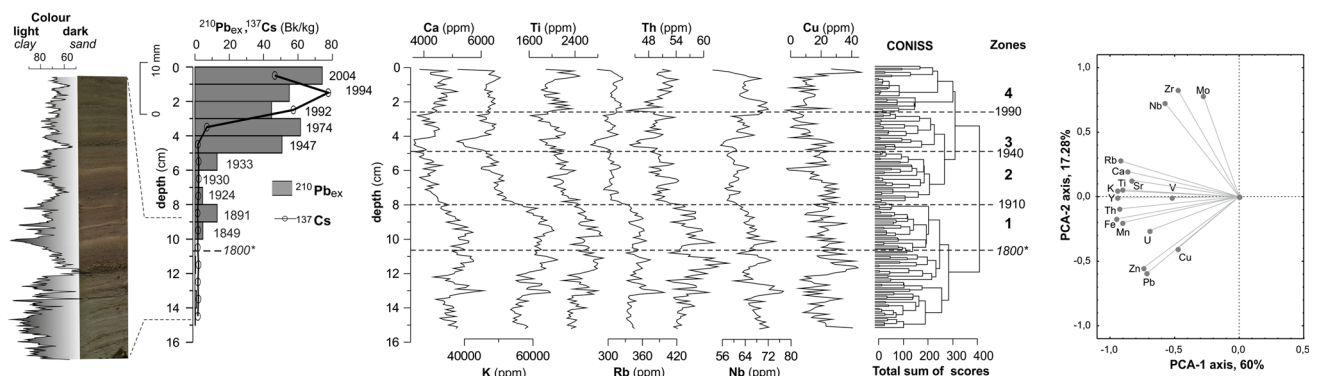
Fig. 3 Core Izumrudnoe (Baikalsky): the depth–age model based on radioactive isotopes ^{210}Pb and ^{137}Cs, the distributions of some elements in the (biplot for the first two principal components, XRF-SR-data)
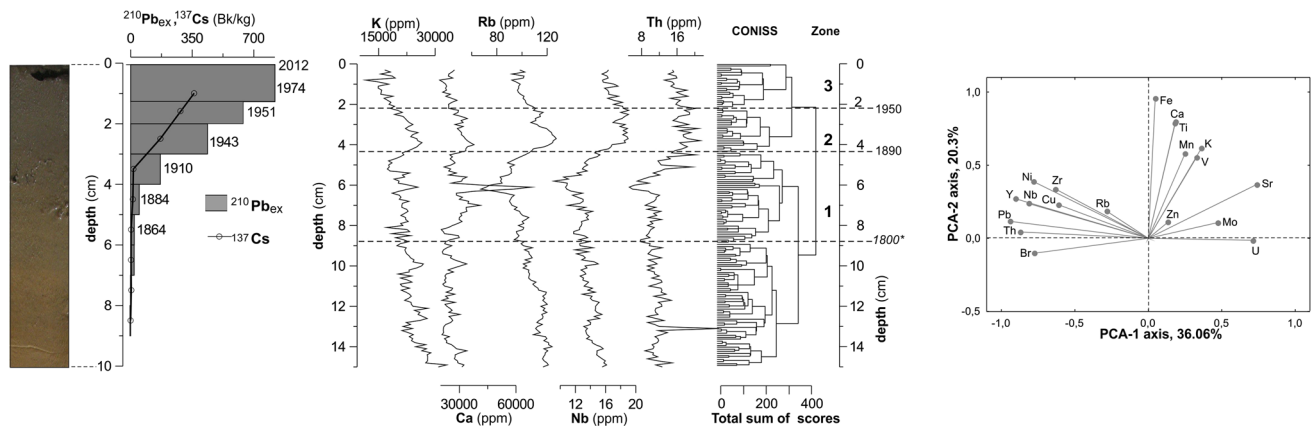
Fig. 4 Core Preobrazhenskoe (Kodar): the depth–age model based on radioactive isotopes ^{210}Pb and ^{137}Cs, the distributions of some elements in the sediments (biplot for the first two principal components, XRF-SR-data)

compounds (Ca, K, Fe and Mn), and Ti most likely incorporated into colloidal iron complexes.

We divided elemental and mineralogical records of the interval core formed in ca. 1800 (0–8.7 cm bss) into three zones (1–3). Zone 1 (8.7–4.3 cm bss, ca. 1800–1890) was characterised by a moderate low content of all elements, except Ca (Fig. 4). There was a tendency to gradually increase elements beginning from ca. 1860. The content of elements of the PCA-2 axis increased more drastically than that of the PCA-1 axis. Zone 2 (4.2–2.2 cm bss, ca. 1890–1950) was characterised by higher content of elements; however, the content of elements of the PCA-2 axis decreased since ca. 1910. In Zone 3 (2.2–0 cm bss, ca. 1950 to the present), the content of practically all analysed elements clearly decreased.

Discussion

In many cases, the distribution of Ca, K, Fe, Mn, Sr, As and other high-mobility elements will be closely associated with the intensity of weathering, leaching and development of soils in the watersheds (e.g., Davison 1993; Gaillardet et al. 2003; Pokrovsky et al. 2006) whereas, the distribution of Rb, Ga, Y, Nb, Ti, Zr or Th will be closely associated with the clastic material primarily transported as suspended particulates (e.g., Nesbitt 1979). Ni, Cu, Br, As and U in lake sediments can be regarded as autochthonous by origin (Phedorin et al. 2000a, b, 2008). However, in our cases, the PCA analyses did not show strong difference in accumulation of these elements. It should be attributed to: (1) there is no large difference in rock and soil types in small watersheds of our glaciers; (2) the continental climate of East Siberia causes minor chemical weathering during warm periods and strong physical weathering during cold periods due to seasonal frost cracking and acceleration of physical

weathering by the glacier flow; (3) poor bioproductivity in proglacial lakes. We assumed that elemental composition of the cores depended on physical weathering, while elements were mainly supplied into proglacial lakes as clastic material.

Fine laminate textures expressed by alternation of clay silt and sand silt layers in bottom sediments most likely showed that the clastic material was supplied by surface inflows. There are two main sources of water supply in proglacial lakes: precipitation and meltwater of glaciers. An elemental record from Lake Ekhoy has high time-resolution. Figure 5 illustrated that annual changes in element distribution link with the clastic material and the sediment rate correlates more closely with changes in summer temperatures than with precipitation. According to the inventory of the glaciers located in East Siberia and based on high-resolution satellite imagery and field investigations, high correlation was established between changes in water balances of glaciers and regional summer temperatures (Shahgedanova et al. 2011; Osipov and Osipova 2014). In our opinion, the intensity of the surface water supply into proglacial lakes primarily depended upon the rate of glaciers' melting and summer air temperature.

We compared our records with the regional climate records (1900–2010), summer air temperature in Europe (Xoplaki et al. 2005) and insolation in the Northern Hemisphere (Steinhilber et al. 2009) for the last 210 years. Figure 6 shows that a tendency in changes of summer temperatures in East Siberia was mainly similar to that in Europe, but these changes were more contrast in East Siberia. Although Peretolchin Glacier is the northward exposition, but the highest sediment rate (mean value 1.8 mm year^{-1}) was recorded in Lake Ekhoy, while the mean values of the sediment rate in Lakes Izumrudnoe and Preobrazhenskoe were about 0.5 mm year^{-1} (Fig. 5). It means that the melting rate of Peretolchin Glacier was

Fig. 5 The result of cluster analyses on distribution of some elements along core Ekhoy (interpolated XRF-SR-data), regional temperature and precipitation (*left panel*), sediment rates calculated (*right panel*) in Lakes Ekhoy (ESR), Izumrudnoe (BR), and Preobrazhenskoe (KR)
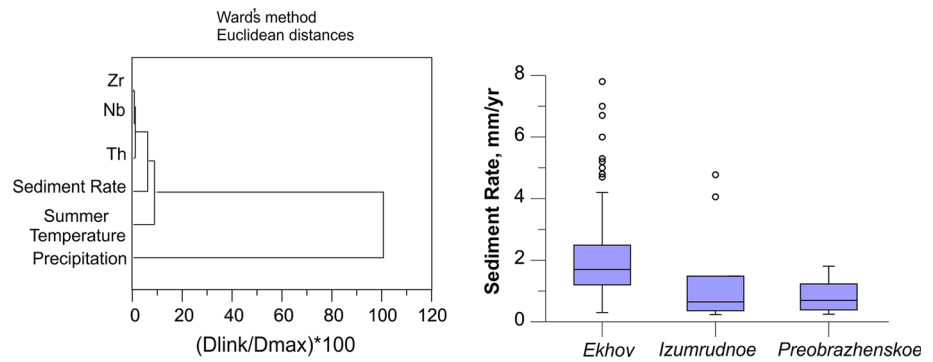
higher than in other East Siberian glaciers. It was unexpected because Peretolchin Glacier is located at a high altitude (2937–3490 m a.s.l), and air temperatures in this area are likely lower than in other studied areas due to the strong altitude effect. For example, the mass balance of this glacier situated at 2800–3000 m a.s.l likely approaches to positive or changes in the thickness vary only between 0 and −20 m (Paul and Haeberli 2008; Machguth et al. 2012). It is most likely that the solar radiation factor is more significant for ESR than for KR and BR. The total annual solar insolation in ESR is up to 5200, whereas in BR and KR it is up to 3800 mJ/m^2 (Sochava 1967; Galazii 1993). The duration of the total solar radiance in ESR was about 2240 h year^{-1}, in BR and KR about 1950 and 1880 h year^{-1}, respectively (Zaloznaya and Postnokova 1966). Liu et al. (2009) have reported a similar assumption that the effect of the global increasing temperature is more pronounced at higher elevations than at lower ones.

The results of the wavelet analysis of the air summer temperatures in Europe (Xoplaki et al. 2005) evidence that short periodical oscillations gradually increase from the beginning of the RW till present (Fig. 6). We also observed in our record the shifting to the short periodical oscillation in the supply of clastic elements into proglacial lakes during the RW (Fig. 6). This tendency was more clearly visualised in the records from Lakes Ekhoy and Izumrudnoe. There were three short episodes (about 1860, 1950 and 1990) in our records and in the record of European summer air temperature when these oscillations were dominated. These episodes occurred closely to boundaries of elemental zones, and they most likely evidenced about changes in water balance of glaciers under summer air temperatures. We defined three significant periods in glacier dynamic regime during the past 210 years (Fig. 6).

The first period from 1800 to 1890. According to many reconstructions of global surface temperatures for the Northern Hemisphere, a transition from the LIA to the recent warming period was characterised by sharp increase in annual temperature that occurred ca. 1850–1860 (e.g., Huang 2004; Moberg et al. 2005; Osborn and Briffa 2006). Most mountain glaciers and small ice caps have been

generally retreating ever since the end of the LIA (IPCC 2001, 2007). For example, from the maximum of the LIA the glaciation of the region lost about 50 % in the Altai and Kodar Mountains (Osipov and Osipova 2014, 2015; Ganyushkin et al. 2015). Over the past 110 years the area of perennial snowfields in the Kuznetsk Alatau Mountains (West Siberia) had reduced by 90 % (Adamenko et al. 2015).

The supply of suspended material by meltwater into Lake Ekhoy was not intense until 1850 and into Lake Preobrazenskoe until 1875. In addition, the response of Kodar glaciers to this transition was sharper than that of Peretolchin Glacier (Fig. 6). We assumed that the maximal melting of Kodar glaciers occurred in about the 1900s. However, the rate of the meltwater supply into Lake Izumrudnoe was high during the LIA and decreased at the transition from the LIA to the RW (Fig. 6). It is most likely attributed to the local effect of Lake Baikal on Chersky Glacier, and to the high precipitation rate in this period. For example, precipitation changes at the weather station East Siberia during the period 1970–2010 were most significant at the "Baikalian" station (Osipov and Osipova 2014).

The second period from 1890 to ca. *1940.* This period was characterised by a decrease in insolation and summer temperatures in Europe and East Siberia (Fig. 6). As a result, the supply of meltwater into Lakes Izumrudnoe and Ekhoy sharply decreased, and moderately into Lake Preobrazenskoe. Even the drastic rise in regional precipitation recorded ca. 1910–1920 did not increase the supply of clastic material into proglacial lakes (Fig. 6). This result indicates that the regional glacier water balance was most likely positive. For instance, some glaciers located in the Tien Shan mountains also had positive cumulative mass balance during 1905–1940 (Liu and Han 1992).

The third period from ca. *1940 till present.* This period coincides with the global increase of surface temperature in the Northern Hemisphere (Rayner et al. 2003; Wilson et al. 2007). According to Stokes et al. (2013), Sygyktiskiy and Kolosov Glaciers (KR) decreased by about 45 and 36 % in exposed glacier ice from 1963 to 2010, but with about 41 and 25 % lost since 1995. However, our records did not
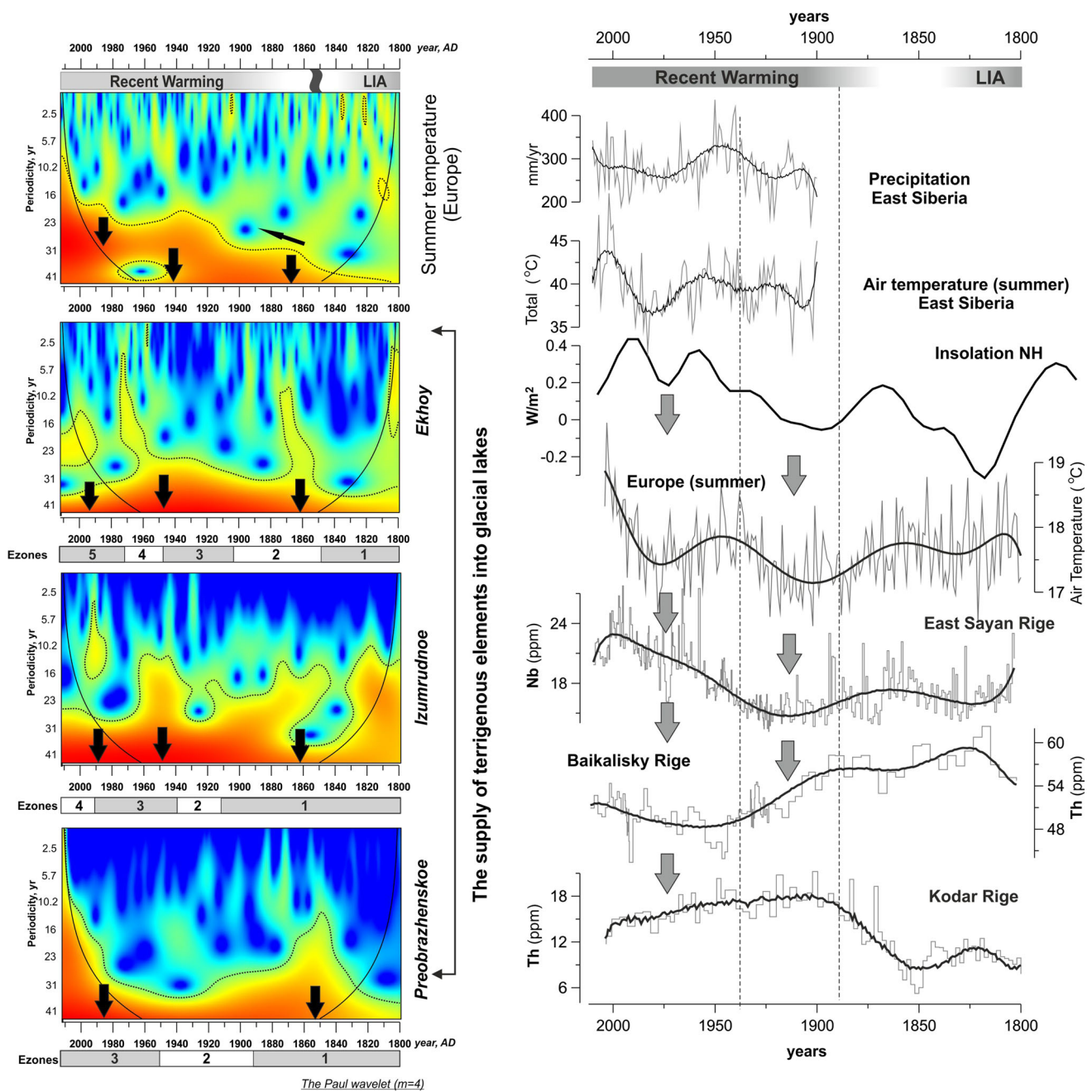
Fig. 6 *Left panel* episodes of short periodical oscillations (*black arrows*) in changes of European air summer temperatures (Xoplaki et al. 2005), from NOAA data-set ftp://ncdc.noaa.gov/pub/data) and supply of clastic elements into proglacial lakes, according the Paul wavelet (*m* = 4), *Ezones* elemental zones. *Right panel* relationships between elemental records from studied proglacial lakes, insolation in the Northern Hemisphere and regional climate parameters (Terrestrial Air Temperature: 1900–2008 Gridded Monthly Time Series, Version 2.01, http://climate.geog.udel.edu), *grey arrows* episodes in decreasing of summer temperature, *vertical dotted lines* three significant periods in dynamic regime of glaciers during the past 210 years

show drastic increase in the supply of clastic material into Lake Preobrazenskoe during the past 50 years; moreover, the supply degreased (Fig. 6). This contradiction should be explained by small exposed areas of this glacier (in 1963 it was about 0.6 km² and in 2010 about 0.33 or 0.38 km²) and effective covering of the surface by debris. As a result, the ablation area of the glacier reduced and the supply of

meltwater into proglacial lakes also decreased. We assumed that these glaciers melted moderately in the period.

Chersky Glacier (BR) showed minimal changes in glacier length and elevation (exposed glacier ice) compared to Kodar and East Sayan glaciers from the end of the LIA to 2011(Osipov and Osipova 2014). The supply of meltwater in Lake Izumrudnoe gradually increased during the third

period and we suppose that the debris covering effect was minor and this glacier reduced rather in thickness than in length. In addition, the increase in snow precipitation over the recent decades (especially since the early 1990s) is a likely explanation of the more moderate glacier shrinkage on the Baikalsky Ridge (Osipov and Osipova 2014).

Peretolchin Glacier (ESR) demonstrated the highest rate of melting and changes in outlines. According to the field-work, the lower outline was situated at 2776 m a.s.l in 1900 (Peretolchin 1908), at 2860 m a.s.l in 1980 (Aref'ev and Mukhametov 1996) and at 2920 m a.s.l in 2006 (Osipov et al. 2013). Our records evidenced that the glacier melted most intensively during 1958–1973 and 1990–2002 (Fig. 6). Similar drastic glaciers' retreat occurred in the South-Western China during 1970–2007 (Li et al. 2011). In addition, according to remote sensing observations, the total area of glacial lakes in the Tibetan Plateau increased by 29.7 % from the 1970s to the 2000s (Song et al. 2014). However, cumulative mass balance of some glaciers located in the Russian Altay Mountains even slightly increased between 1990 and 1998 (WGMS 2011). The melting rate of Peretolchin Glacier drastically decreased since 2002, although it is still high. Interestingly, similar decrease in the supply of clastic material into Lakes Izumrudnoe and Preobrazhenskoe occurred also since 2000. It is most probably that East Siberian glaciers adapted to climate conditions of the last decades. Slowdown of the glacier reduce have been also observed in other parts of Central Asia since the 2000s. Total number of glacial lakes decreased by 45.86 % in the Central China and Nepal Himalayas from 2000 to 2009 (Shijin and Tao 2014).

Compared to other records, the records from bottom sediments of Lake Ehoy correlated more closely with changes in air summer temperatures in Europe and East Siberia and with insolation. We assume that during the last 210 years Peretolchin Glacier is more likely sensitive to temperature changes and melt more intensively compared to Chersky, Sygyktiskiy and Kolosov Glaciers. This result contradicts the glacier inventory based on satellite imagery that glaciers at lower elevations tend to shrink more intensively (e.g., Osipov and Osipova 2014; Li and Li 2014). If this contradiction should be explained by some mistakes in area calculation due to the effective debris covering of small glaciers, an estimate of glacier dynamic over the discharge of meltwater into proglacial lakes should be more informative and has a high time-resolution.

Conclusion

We reconstructed fluctuations of the glaciers located in East Siberia (the East Sayan, Baikalsky and Kodar Ridges), Russia, for the last 210 years based on the data of X-ray

fluorescent technique with synchrotron radiation (step sampling 1 mm) and inductively coupled plasma mass spectrometry from bottom sediments of the proglacial Lakes Ekhoy, Izumrudnoe and Preobrazhenskoe. The depth–age model of the cores was constructed from ^{210}Pb and ^{137}Cs chronology and counting of annual layers. The studied interval of the cores formed during the transition from the LIA to the RW. The intense glacial flow was calculated from the level of terrigenous and leached elements supplied by meltwater into these proglacial lakes. The melting rate of Peretolchin Glacier was higher than that of other East Siberian glaciers. We compared our records with the regional climate records and proxy global climate forcing factors (total solar irradiance). We defined three periods of significant increased glacier flow/melting during the last 210 years. These periods are generically correlated with the positive temperature anomalies. The first period (ca. 1800–1890) was induced by a sharp increase in solar irradiance and annual temperature that occurred in the Northern Hemisphere in ca. 1850–1860. The supply of suspended material by meltwater into Lake Ekhoy was not intense until 1850 and into Lake Preobrazhenskoe until 1875. However, the rate of meltwater supply into Lake Izumrudnoe was high during the LIA and decreased at a transition from the LIA to the RW. During the second period (ca. 1890–1940), the supply of meltwater into Lakes Izumrudnoe and Ekhoy sharply decreased, and moderately in Lake Preobrazenskoe. We assume the regional glacier water balance was most likely positive. In the third period (ca. 1940-till present), the melting rates of glaciers located on KR and BR were moderate, in contrast to Peretolchin Glacier (ESR) that demonstrated the highest rate of melting and changes in outlines during this period. However, the melting rate of Peretolchin Glacier drastically decreased since 2002.

References

Adamenko MM, Gutak YaM, Solomina ON (2015) Glacial history of the Kuznetsky Alatau mountains. TI Glacier in Asia. Environ Earth Sci: (in last revision)

Aleshin GV (1982) Modern glaciers and their significance for relief formation of the Baikalsky Ridge. Geogr Nature Res 4:133–136 **(in Russian)**

An Z (2000) The history and variability of the East Asian paleomonsoon climate. Quat Sci Rev 19:171–187

Aref'ev VE, Mukhametov RM (1996) On the glaciers of the Altai and Sayan. Barnaul (**In Russian**)

Avsiuk GA, Kotlyakov VM (1967) Mountain glaciation in the U.S.S.R.; extension, classification and ice storage in glaciers. In: Hirobumi O (ed) Physics of snow and ice. Hokkaido Univ Inst, Low Temp Sci, Hokkaido, pp 389–394

Back S, Strecker MR (1998) Asymmetric late Pleistocene glaciations in the North Basin of the Baikal Rift, Russia. J Geol Soc 155:61–69

Bakke J, Lie Ø, Nesje A, Dahl SO, Paasche Ø (2005) Utilizing physical sediment variability in glacier-fed lakes for continuous glacier reconstructions during the Holocene, northern Folgefonna, western Norway. The Holocene 15:161–176

Binford MW (1990) Calculation and Uncertainty Analysis of ^{210}Pb Dates for PIRLA project cores. J Paleolimnol 3:253–267

Carrivick JL, Tweed FS (2013) Proglacial lakes: character, behaviour and geological importance. Quat Sci Rev 78:34–52

Dahl SO, Bakke J, Lie O, Nesje A (2003) Reconstruction of former glacier equilibrium-line altitudes based on proglacial sites: an evaluation of approaches and selection of sites. Quat Sci Rev 22:275–287

Davison W (1993) Iron and manganese in lakes. Earth Sci Rev 34:119–163

Dyurgerov MB, Meier MF (2000) Twentieth century climate change: evidence from small glaciers. Natl Acad Sci 97:1406–1411

Galazii GI (1993) Atlas of Baikal. Roskartografia, Moscow (**In Russian**)

Gaillardet J, Viers J, Dupre B (2003) Treatise on Geochemistry. In: Holland HM, Turekian KK (eds) Elsevier Pergamon, Oxford 5:225–272

Ganyushkin DA, Chistyakov FV, Kunaeva EP (2015) Fluctuation of glaciers in the south-east Russian Altai and north-west Mongolia mountains since the little ice age maximum. TI Glacier in Asia. Environ Earth Sci. doi:10.1007/s12665-015-4301-2

Gardelle J, Arnaud Y, Berthier E (2011) Contrasted evolution of glacial lakes along the Hindu Kush Himalaya mountain range between 1990 and 2009. Glob Planet Chang 75:47–55

Gavshin VM, Melgunov MS, Sukhorukov FV, Bobrov VA, Kalugin IA, Klerkx J (2005) Disequilibrium between uranium and its progeny in the Lake Issyk-Kul system (Kyrgyzstan) under a combined effect of natural and manmade processes. J Environ Radioact 83:61–74

Haeberli W, Frauenfelder R, Kääb A, Wagner S (2004) Characteristics and potential climatic significance of "miniature ice caps" (crest- and cornice-type low-altitude ice archives). J Glaciol 50:129–136

Hoelzle M, Chinn T, Stumm D, Paul F, Zemp M, Haeberli W (2007) The application of glacier inventory data for estimating past climate change effects on mountain glaciers: a comparison between the European Alps and the Southern Alps of New Zealand. Glob Planet Chang 56:69–82

Huang S (2004) Merging information from different resources for new insights into climate change in the past and future. Geophys Res Lett. doi:10.1029/2004GL019781

IPCC (2001) Intergovernmental Panel on Climate Change. Climate Change 2001: The Scientific Basis. Contribution of Working Group II to the Third Assessment Report of the Intergovernmental Panel on Climate Change. Cambridge University Press, Cambridge

IPCC (2007) Intergovernmental Panel on Climate Change. IPCC Fourth Assessment Report: climate change 2007. Synthesis Report (AR4). World Meteorological Organization (WMO) and United, Geneva

Jones PD, Briffa KR, Osborn TJ, Lough JM, van Ommen TD, Vinther BM, Luterbacher J, Wahl E, Zwiers FW, Mann ME, Schmid GA, Ammann CM, Buckley BM, Cobb KM, Esper J, Goosse H, Graham N, Jansen E, Kiefer T, Kull C, Küttel M, Mosley-Thompson E, Overpeck JT, Riedwyl N, Schulz M, Tudhope AW, Villalba R, Wanner H, Wolff E, Xoplaki E (2009) High-resolution palaeoclimatology of the last millennium: a review of current status and future prospects. The Holocene 19:3–49

Juggins S (2012) rioja: Analysis of quaternary science data, R package version (0.8-5). http://cran.r-project.org/package=rioja

Karlen W, Matthews J (1992) Reconstructing Holocene glacier variations from glacier lake sediments: studies from Nordvestlandet and Jostedalsbreen-Jotunheimen, southern Norway. Geog Ann 63A:273–281

Kitov AD, Kovalenko SN, Plusnin VM (2009) Results of the 100-year observations of the dynamics of glacial geosystems of Munch-Sardyk massif. Geogr Natur Res 3:101–108

Kuznetsova LP (1978) Transfer of moisture over the territory of the USSR. Nauka, Moscow (In Russian)

Larsen DJ, Miller GH, Geirsdóttir Á, Thordarson T (2011) A 3000-year varved record of glacier activity and climate change from the proglacial lake Hvítárvatn, Iceland. Quat Sci Rev 30:2715–2731

Li Z, He Y, An W, Song L, Zhang W, Catto N, Wang Y, Wang S, Liu H, Cao W, Theakstone WH, Wang S, Du J (2011) Climate and glacier change in southwestern China during the past several decades. Environ Res Lett 6(045404):24

Lie O, Dahl SO, Nesje A, Matthews JA, Sandvold S (2004) Holocene fluctuations of a polythermal glacier in high-alpine eastern Jotunheimen, central-southern Norway. Quat Sci Rev 23:1925–1945

Liu C, Han T (1992) Relation between recent glacier variations and climate in the Tien Shan mountains, central Asia. Ann Glaciol 16:11–16

Liu XD, Cheng ZG, Yan LB, Yin ZY (2009) Elevation dependency of recent and future minimum surface air temperature trends in the Tibetan Plateau and its surroundings. Glob Planet Chang 68(3):164–174

Machguth H, Haeberli W, Paul F (2012) Mass-balance parameters derived from a synthetic network of mass-balance glaciers. J Glaciol 58(211):965–979

Margold M, Jansson KN (2011) Glacial geomorphology and glacial lakes of central Transbaikalia, Siberia, Russia. J Maps 7:18–30

Melgunov MS, Gavshin VM, Sukhorukov FV, Kalugin IA, Bobrov VA, Klerkx J (2003) Anomalies of radioactivity on the southern bank of the Ysyk-Köl Lake (Kyrgyzstan). Chem Sustain Dev 11:859–870 (In Russian)

Moberg A, Sonechkin DM, Holmgren K, Datsenko NM, Karlen W (2005) Highly variable Northern Hemisphere temperatures reconstructed from low and high-resolution proxy data. Nature 433:613–617

Ndiaye M, Davaud E, Ariztegui D, Fall M (2012) Int J Geosci 3:206

Nesbitt HW (1979) Mobility and fractionation of rare earth elements during weathering of a granodiorite. Nature 279:206–210

Nesje A, Dahl SO (2001) The Greenland 8200 cal. year BP event detected in loss-on-ignition profiles in Norwegian lacustrine sediment sequences. J Quat Sci 16:155–166

Nesje A, Bakke J, Dahl SO, Lie O, Matthews JA (2008) Norwegian mountain glaciers in the past, present and future. Glob Planet Chang 60:1–27

Nie Y, Zhang Y, Ding M, Liu L, Wang Z (2013) Lake change and its implication in the vicinity of Mt. Qomolangma (Everest), central high Himalayas, 1970–2009. Environ Earth Sci 68:251–265

Osborn TJ, Briffa KR (2006) The spatial extent of 20th century warmth in the context of the past 1200 years. Science 311:841–844

Osipov EY, Khlystov OM (2010) Glaciers and meltwater flux to Lake Baikal during the Last Glacial Maximum. Palaeogeog Palaeoclim Palaeoecol 294:4–15

Osipov EY, Osipova OP (2014) Mountain glaciers of southeast Siberia: current state and changes since the Little Ice Age. Ann Glaciol 55(66):167–176

Osipov EY, Osipova OP (2015) Glaciers of the Levaya Sygykta River watershed, Kodar Ridge, southeastern Siberia, Russia: modern morphology, climate conditions and changes over the past decades. TI Glacier in Asia. Environ Earth Sci. doi:10.1007/s12665-015-4352-4

Osipov EY, Grachev MA, Mats VD, Khlystov OM, Breitenbach S (2003) Mountain glaciers of the Pleistocene Last Glacial Maximum in the northwestern Barguzin Range (Northern Baikal Region): paleoglacial reconstruction. Russ Geol Geophys 44:652–663

Osipov EY, Ashmetev AY, Osipova OP, Klevtsov (2013) New glacier inventory of the south-east part of Eastern Sayan. Ice Snow 3:123 (In Russian)

Owen LA, Thackray G, Anderson RS, Briner J, Kaufman D, Roe G, Yi C (2009) Integrated research on mountain glaciers: current status, priorities and future prospects. Geomorphology 103(2):158–171

Paul F (2002) Changes in glacier area in Tyrol, Austria, between 1969 and 1992 derived from Landsat 5 Thematic Mapper and Austrian Glacier Inventory data. Remote Sens 23:787–799

Paul F, Haeberli W (2008) Spatial variability of glacier elevation changes in the Swiss Alps obtained from two digital elevation models. Geophys Res Lett 35:L21502. doi:10.1029/2008GL034718

Peretolchin SP (1908) Glaciers of the Munku-Sardyk ridge. Izvestiia Tomsk Technol Inst 9(1):47

Phedorin MA, Goldberg EL (2005) Prediction of absolute concentrations of elements from SR XRF scan measurements of natural wet sediments. Nucl Instrum Methods Phys Res A 543:274–279

Phedorin MA, Bobrov VA, Goldberg EL, Navez J, Zolotaryov KV, Grachev MA (2000a) SR-XFA as a method of choice in the search of signals of changing palaeoclimates in the sediments of Lake Baikal, compared to INAA and ICP-MS. Nucl Instrum Methods Phys Res A 448:394–399

Phedorin MA, Goldberg EL, Grachev MA, Levina OL, Khlystov OM, Dolbnya IP (2000b) The comparison of biogenic silica, Br and Nd distributions in the sediments of Lake Baikal as proxies of changing paleoclimates of the last 480 ky. Nucl Instrum Methods Phys Res A 448:400–406

Phedorin MA, Fedotov AP, Vorobieva SS, Ziborova GA (2008) Signature of long supercycles in the Pleistocene history of Asian limnic systems. J Paleolimnol 40:445–452

Plyusnin VM, Drozdova OV, Kitov AD, Kovalenko SN (2008) The dynamics of mountain geosystems in southern Siberia. Geogr Nat Res 2:5–14

Pokrovsky OS, Schott J, Dupre B (2006) Trace element fractionation and transport in boreal rivers and soil porewaters of permafrost-dominated basaltic terrain in Central Siberia. Geochim Cosmochim Acta 70:3239–3260

Preobrazhenskiy VS (1960) Kodar Glacial Area (Transbaikalia). IX section of the International Geophysical Year Program (Glaciology). Published by the Academy of Sciences of the USSR, Moscow (In Russian)

Rayner NA, Parker DE, Horton EB, Folland CK, Alexander LV, Rowell DP, Kent EC, Kaplan A (2003) Global analyses of SST, sea ice and night marine air temperature since the late nineteenth century. J Geophys Res 108(D14):4407. doi:10.1029/2002JD002670

Rosqvist G, Jonsson C, Yam R, Karlen W, Shemesh A (2004) Diatom oxygen isotopes in pro-glacial lake sediments from northern Sweden: a 5000 year record of atmospheric circulation. Quat Sci Rev 23:851–859

Shahgedanova M, Popovnin V, Aleynikov A, Stokes CR (2011) Geodetic mass balance of Azarova glacier, Kodar Mountains, eastern Siberia, and its links to observed and projected climatic change. Ann Glaciol 52:129–137

Shijin W, Tao Z (2014) Spatial change detection of glacial lakes in the Koshi River Basin, the Central Himalayas. Environ Earth Sci 72:4381–4391

Sochava VB (1967) Atlas of Transbaikalia. GUGK, M-Irkutsk (In Russian)

Solomina ON (2000) Retreat of mountain glaciers of northern Eurasia since the Little Ice Age maximum. Ann Glaciol 31:26–30

Solomina O, Haeberli W, Kull C, Wiles G (2008) Historical and Holocene glacier–climate variations: general concepts and overview. Glob Planet Chang 60:1–9

Song C, Huang B, Ke L, Richards KS (2014) Remote sensing of alpine lake water environment changes on the Tibetan Plateau and surroundings: A review. ISPRS J Photogramm Remote Sens 92:26–37

Steinhilber F, Beer J, Fröhlich C (2009) Total solar irradiance during the Holocene. Geophys Res Lett. doi:10.1029/2009GL040142

Stoetter J, Wastl M, Caseldine C, Haberle T (1999) Holocene palaeoclimatic reconstruction in northern Iceland: approaches and results. Quat Sci Rev 18:457–474

Stokes CR, Shahgedanova M, Evans IS, Popovnin VV (2013) Accelerated loss of alpine glaciers in the Kodar Mountains, south-eastern Siberia. Glob Planet Chang 101:82–96

Trounova VA, Zolotarev KV, Baryshev VB, Phedorin MA (1998) Analytical possibilities of SRXRF station at VEPP-3 SR-source. Nucl Instrum Methods Phys Res A 405:532–536

Vorobyeva SS, Trunova VA, Stepanova OG, Zvereva VV, Petrovskii SK, Melgunov MS, Zheleznyakova TO, Chechetkina LG, Fedotov AP (2015) Impact of glacier changes on ecosystem of proglacial lakes in high mountain regions of East Siberia (Russia). TI Glacier in Asia. Environ Earth Sci. doi:10.1007/s12665-015-4164-6

Wang N, Wu H, Wu Yu, Chen A (2015) Variations of the glacier mass balance and lake water storage in the Tarim Basin, northwest China, over the period of 2003–2009 estimated by the ICESat-GLAS data. Environ Earth Sci. doi:(in last revision)

WGMS (2011) Glacier Mass Balance Bulletin No. 11 (2008–2009). In: Zemp M, Nussbaumer SU, Gärtner-Roer I, Hoelzle M, Paul F, Haeberli W (eds) ICSU(WDS)/IUGG(IACS)/UNEP/UNESCO/WMO. World Glacier Monitoring Service, Zurich, p 102

Wilson R, D'Arrigo R, Buckley B, Büntgen U, Esper J, Frank D, Luckman B, Payette S, Vose R, Youngblut D (2007) A matter of divergence: tracking recent warming at hemispheric scales using tree ring data. J Geophys Res 112:D17103. doi:10.1029/2006JD008318

Xoplaki E, Luterbacher J, Paeth H, Dietrich D, Steiner N, Grosjean M, Wanner H (2005) European spring and autumn temperature variability and change of extremes over the last half millennium. Geophys Res Lett. doi:10.1029/2005GL023424

Ya Li, Yi Li (2014) Topographic and geometric controls on glacier changes in the central Tien Shan, China, since the Little Ice Age. Ann Glaciol 55(66):177–186

Yang B, Bräuning A, Dong Z, Zhang Z, Keqing J (2008) Late Holocene monsoonal temperate glacier fluctuations on the Tibetan Plateau. Glob Planet Chang 60:126–140

Zaloznaya VI, Postnikova NG (1966) Climate Handbook USSR. Gidrometeoizdat, Leningrad (In Russian)

Zhao QD, Ye BS, Ding YJ, Zhang SQ, Yi SH, Wang J, Shangguan DH, Zhao CC, Han HD (2013) Coupling a glacier melt model to the Variable Infiltration Capacity (VIC) model for hydrological modeling in north-western China. Environ Earth Sci 68:87–101

Zhuchenko NA, Chebykin EP, Stepanova OG, Chebykin AP, Gol'dberg EL (2008) Microwave digestion of bottom sediments from Lake Baikal for the inductively coupled plasma mass-spectrometric determination of their elemental composition. J Anal Chem 63:943–949

Zolotarev KV, Goldberg EL, Kondratyev VI, Kulipanov GN, Miginsky EG, Tsukanov VM, Phedorin MA, Kolmogorov YP (2001) Scanning SR-XRF beamline for analysis of bottom sediments. Nucl Instrum Methods Phys Res A 470:376–379